Hansen Bow[1]
Jianping Fu[2]
Jongyoon Han[1,3]

[1]Department of Electrical Engineering and Computer Science, Massachusetts Institute of Technology, Cambridge, MA, USA
[2]Department of Mechanical Engineering, Massachusetts Institute of Technology, Cambridge, MA, USA
[3]Department of Biological Engineering, Massachusetts Institute of Technology, Cambridge, MA, USA

Received April 20, 2008
Revised July 31, 2008
Accepted August 22, 2008

Research Article

Decreasing effective nanofluidic filter size by modulating electrical double layers: Separation enhancement in microfabricated nanofluidic filters

Conventional methods for separating biomolecules are based on steric interactions between the biomolecules and randomly oriented gel fibers. The recently developed artificial molecular sieves also rely on steric interactions for separation. In this work, we present an experimental investigation of a method that can be used in these sieves to increase separation selectivity and resolution. This method exploits the electrostatic repulsion between the charged molecules and the charged nanofluidic structure. Although this method has been mentioned in the previous work, it has not been examined in detail. We characterize this method by comparing the selectivity with that achieved in devices with different dimensions. The results of this study are relevant to the optimization of chip-based gel-free biomolecule separation and analysis.

Keywords:
Debye length / DNA / Electrostatic / Microfluidic / Nanofluidic
DOI 10.1002/elps.200800256

1 Introduction

The ability to quickly and efficiently separate biologically relevant molecules is necessary for diagnostic, screening, and research purposes. Recently, Fu *et al.* have introduced a gel-free nanofluidic filter (nanofilter) array that is able to rapidly separate short dsDNA and proteins [1]. Under moderate electric field strength E, the separation mechanism involves repeated partitioning between a relatively unconstrained deep region and a constricted shallow region [2]. Because smaller molecules partition into the shallow region more frequently than larger ones, their migration velocity V and therefore electrophoretic mobility μ ($\mu = V/E$) are of greater values. Compared with conventional methods of separating DNA and proteins, such as gel electrophoresis and HPLC, the nanofilter array offers benefits of speed, lower reagent consumption, ease of target molecule collection, and reusability.

Although the gel-free separation of DNA and proteins using microfabricated nanofilters has been demonstrated [1], the separation resolution of this approach is limited in part by how narrow the constricted shallow regions can be made [3]. The available theoretical model has demonstrated that size selectivity is inversely proportional to the nanofilter shallow region depth [2]. Fabrication and experimental limitations include the collapse of the structure during anodic bonding and the inability to fill the device with buffer solution, especially when the nanofilter gap size is made to be smaller than about 10 nm. These factors have prevented further improvement of size selectivity and separation resolution by simply decreasing the nanofilter gap size.

We show that one can effectively increase the separation selectivity of the nanofilters by exploiting the strong electrostatic repulsion between the charged nanofilter walls and charged biomolecules. By decreasing the buffer ionic strength, the electrostatic repulsion between the negatively charged nanofilter walls and the negatively charged DNA starts to affect the partitioning of the molecules between the deep and shallow regions. Although the depth of the shallow region is physically the same, the electrostatic repulsion effectively reduces the shallow region depth for negatively charged molecules, therefore enhancing the size selectivity and separation resolution. Early studies using semipermeable membranes and polymeric gels have clearly demonstrated the effects of ionic strength on hindered diffusive and convective solute transport [4–6]. However, these previous studies of ionic strength effects were performed using either membranes that were radioactive track-etched [4] or polymeric gels [5]. The track-etched membranes provide many randomly distributed pores arranged in parallel, in contrast to our system, which provides pores in

Correspondence: Associate Professor Jongyoon Han, Department of Electrical Engineering and Computer Science, Massachusetts Institute of Technology, Room 36-841, 77 Massachusetts Avenue, Cambridge, MA 02139, USA
E-mail: jyhan@mit.edu
Fax: +1617-258-5846

Abbreviation: nanofilter, nanofluidic filter

series. For gels, it is difficult to precisely determine the distance between the gel fibers, which is necessary to determine the partition coefficient. More importantly, different ionic strengths can affect the structure of the gel itself [7]. In contrast to previous studies using gels and membranes, we believe that our precisely microfabricated nanofilter system provides a well-characterized environment to study electrostatic interactions between the solutes and the rigid walls of the device, which will potentially aid in improving the design and operation of future nanofilter devices.

The electrostatic sieving effect of native proteins through a two-dimensional nanofilter array was briefly studied in Fu *et al.* [8]. In that study, differently charged proteins of similar size were used. Although that study introduced the idea of electrostatic effects on charge selectivity in a two-dimensional array, no attempt to theoretically model that effect or to provide any quantification of the experimental results was provided. The inability to model or quantify the experimental observations may be attributed to several reasons. Due to the proteins' difference in charge/hydrodynamic drag ratio, they should exhibit different electrophoretic mobilities. According to Fu *et al.* the energy barrier for these proteins to enter the constrained region is different, even in high ionic strength conditions [2]. Additionally, proteins are inherently difficult molecules to study due to their non-uniform charge density and irregular shapes. Lastly, molecular movement in a two-dimensional filter array is inherently more difficult to characterize due to two simultaneous forces acting parallel and perpendicular to the nanofilter constriction.

In contrast to that study, in this work we present a more rigorous study of the electrostatic sieving effect using short, linear DNA molecules in a one-dimensional nanofilter device. Short DNA fragments have a well-characterized conformation (rod-like, with a persistence length of around 50 nm (150 bp)), constant charge-to-mass ratio, and size-independent free-solution electrophoretic mobility [9]. These characteristics of DNA make it an ideal model molecule to study the electrostatic sieving effect across the nanofilter. In addition to the experiments involving different ionic strengths, we provide control experiments using devices with different deep and shallow regions created by the fabrication process and devices with only a flat, filter-less nanochannel. We also provide a theoretical quantification of the experimental observations using the DNA effective diameter [10], surface potential, and Debye screening length.

2 Materials and methods

Figure 1A and B are the top and the side view schematic of the device, respectively. Details regarding device fabrication have been described previously [11]. A Hamamatsu Model C4742-80-12AG CCD camera (Hamamatsu Photonics, Japan), connected to an inverted epi-fluorescent Olympus IX71 (Olympus, Center Valley, PA, USA) microscope, was used for imaging. A 488 nm argon-ion laser provided illumination. Voltage was provided by a Labsmith HVS448 3000D (Labsmith, Livermore, CA, USA) voltage source connected to platinum electrodes. dsDNA ladder samples were purchased from New England BioLabs (Beverly, MA, USA). They were labeled with the intercalating fluorescent dye YOYO-1 (Molecular Probes, Eugene, OR, USA) in TBE 5 ×, 1 ×, or 0.25 × buffer. TBE 5 × consists of 0.445 M Tris–borate and 10 mM EDTA at pH ~8.3. The other TBE concentrations were created by diluting TBE 5 × with DI water. The dye to DNA bp ratio was about 1:10 and the final DNA concentration was about 12.8 μg/mL. TBE 5 ×, 1 ×, or 0.25 × buffer, respectively, was also used as the electrophoresis buffer inside the nanofilter arrays. Electroosmotic flow at 100 V/cm was performed overnight with the new

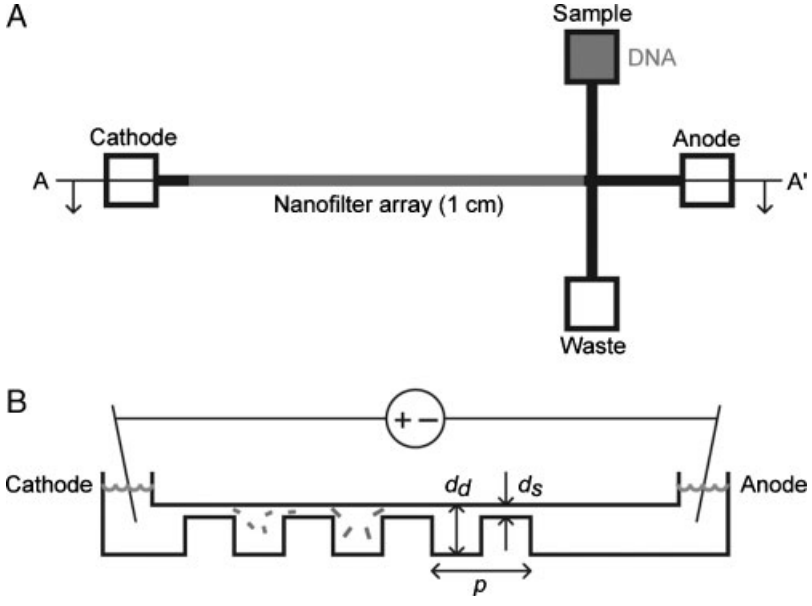

Figure 1. Schematic of the nanofilter array. (A) Device layout. (B) Schematic cross-section through A–A′. An electric field in the nanofilter region causes shorter DNA molecules to travel faster.

buffer in the event of a buffer change. The reservoirs were covered by paraffin wax, which made buffer evaporation negligible. Peak fitting was done using Origin 7 software (OriginLab, Northampton, MA, USA).

3 Results and discussion

3.1 Theory

The following is a concise summary of the relevant ideas presented in [2]. The theory presented here has been simplified to eliminate details that do not affect the present study. The free-energy barrier at the abrupt interface between the nanofilter deep and shallow regions originates from the limited configurational freedom inside the shallow region (*i.e.* configurational entropy loss) caused by the steric constraints imposed by the nanofilter walls. Therefore, entry into the restricted nanofilter shallow region can only be realized if the DNA molecules are properly positioned and oriented without overlapping the nanofilter wall. The configurational entropic barrier can be calculated based on DNA partitioning between the deep and the shallow regions as $-T\Delta S^0 \sim -k_B T \ln \Omega_s/\Omega_d$ (T is the absolute temperature, S^0 the configurational entropy, k_B Boltzmann's constant, and Ω_s/Ω_d the ratio of permissible configuration state integrals between shallow and deep regions) [2]. By definition, Ω_s/Ω_d equals K ($K = K_s/K_d$), the ratio of the partition coefficients in the shallow (K_s) and the deep regions (K_d).

We can calculate the DNA partition coefficient K_i in the shallow ($i = s$) and the deep regions ($i = d$) by treating short DNA as thin rod-like molecules with end-to-end length L: the contour lengths of 50–500 bp DNA (approximately 17–170 nm) are comparable to the DNA persistence length ($l_p = 50$ nm). From the Kratky–Porod model (worm-like chain model), the end-to-end distance L of the DNA molecules is

$$L = \langle R^2 \rangle^{1/2} = \left\{ 2ll_p \left[1 - \frac{l_p}{l} \left\{ 1 - \exp\left(-\frac{l}{l_p} \right) \right\} \right] \right\}^{1/2} \quad (1)$$

Based on geometrical and statistical arguments, the partition coefficients K_i ($i = s, d$) of rod-like DNA in the dilute solution limit for both the shallow and deep regions are approximately [12]

$$K_i = 1 - \tfrac{1}{2}\beta_i \quad (\beta_i \leq 1)$$

$$K_i = \frac{1}{2\beta_i} \quad (1 \leq \beta_i) \quad (2)$$

where $\beta_i = L/d_i$ (scaled molecular length).

The relative mobility μ^* of DNA through the nanofilter array can be written as

$$\mu^* = \frac{\mu}{\mu_{max}} \quad (3)$$

where μ is the DNA mobility in the nanofilter array and μ_{max} is the maximum sieving-free mobility. All the nanofilters tested in the paper consist of equal deep and shallow region lengths; therefore, $\mu_{max} = 4d_s d_d \mu_0/(d_s + d_d)^2$, where μ_0 is the DNA free-solution mobility. The DNA mobility μ has been theoretically calculated based on the equilibrium partitioning theory and the Kramers rate theory [2] and, to a first-order approximation, the relative mobility μ^* of a DNA molecule is approximately equal to its partition coefficient in the shallow region as $\mu^* \cong K_s$.

3.2 Influence of physical dimensions on selectivity

In Fig. 2A, we compared the relative mobility μ^* of the 100 bp DNA ladder in two nanofilter arrays with different shallow region depths d_s, but with the ratio of shallow and deep region depths d_s/d_d preserved. For a given electric field E_{av}, the nanofilter arrays with the same d_s/d_d value have the same electric field distributions across the shallow and deep regions; therefore, the maximum sieving-free mobility μ_{max} should be of the same value. The only difference between the two nanofilter devices was the partition coefficient K between the nanofilter shallow and deep regions. The entropic barrier height at the nanofilter constriction rises with decreasing nanofilter shallow region depth d_s. In addition, decreasing d_s results in K_s and K being more dependent on the DNA bp number N ($dK_s/dN \sim -1/d_s$). Therefore, the nanofilter array should exhibit greater size selectivity with shallower nanofilter shallow region d_s. Intuitively, changing the nanofilter shallow region depth alters the number of allowable configuration states inside the nanofilter shallow region. Decreasing d_s lowers the number of allowable configuration states more for longer DNA molecules than shorter ones, resulting in increased selectivity. In our experiments, the separation selectivity increased when we decreased d_s from 80 to 60 nm, Fig. 2A. Decreasing d_s further to 40 nm resulted in difficulty in getting DNA to enter the nanofilter sieving region and fluorescence intensities at the detection region too faint to measure.

Increasing deep region depth d_d did not result in an appreciable change in the nanofilter size selectivity, although similar separations of the same DNA sample took longer to finish, Fig. 2B. The respective elution times for a $d_s = 60$ nm, $d_d = 480$ nm nanofilter array were 1.8 times greater than those for a $d_s = 60$ nm, $d_d = 240$ nm nanofilter array under all electric field conditions, which is consistent with the fact that the maximum sieving-free mobility μ_{max} for the nanofilter array ($d_s = 60$ nm, $d_d = 240$ nm) is about 1.63 times greater than that for the nanofilter array ($d_s = 60$ nm, $d_d = 480$ nm). In the limit of large d_d, $K_d \approx 1$ and $K \approx K_s$, which results in the best selectivity for a given d_s. However, increasing d_d from 240 to 480 nm for the $d_s = 60$ nm device did not improve selectivity appreciably, because $K_d \approx 1$ already for the short DNA molecules in the experiments. More specifically, using Eq. (2) K_d differs by 1.7% at 50 bp and 9% at 300 bp for $d_d = 240$ and 480 nm for a fixed $d_s = 60$ nm. These differences in K_d result in minor selectivity differences, which is consistent with our experimental observations, Fig. 2B.

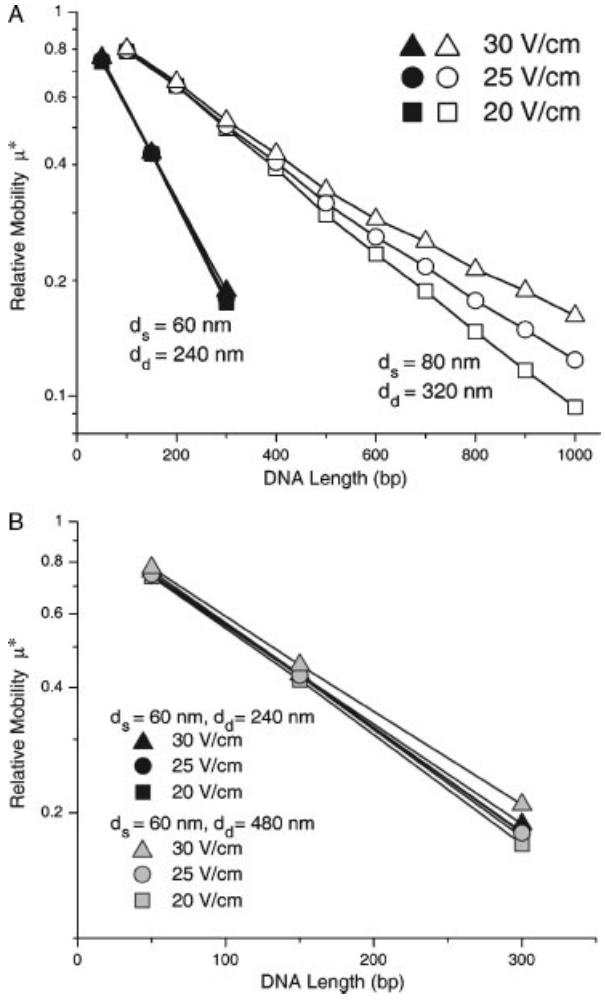

Figure 2. Relative mobility. (A) DNA relative mobility *versus* size for two different d_s's, while the ratio of d_s to d_d was fixed. The dimensions of one device were $d_s = 60$ nm, $d_d = 240$ nm. Those of the other device were $d_s = 80$ nm, $d_d = 320$ nm. (B) DNA relative mobility *versus* size in devices differing only in d_d, where $d_s = 60$ nm. The standard deviations of the mobility are all less than 6%, with most ranging from 2 to 4%, and are hence not included in the figure.

3.3 Influence of buffer ionic strength on selectivity

Decreasing the buffer ionic strength resulted in markedly increased selectivity using the nanofilter arrays, Fig. 3A and b. Experiments in a $d_s = 85$ nm nanofilter device run with TBE 0.25 ×, Fig. 3B, resulted in similar selectivity as those in a $d_s = 60$ nm nanofilter device run with TBE 5 ×, Fig. 2A. Lowering buffer ionic strength accentuates the electrostatic repulsion between the negatively charged walls of the device and the negatively charged DNA. This increased electrostatic repulsion effectively decreases d_s, leading to better selectivity in a similar way as physically decreasing d_s, Fig. 3C. The electrostatic repulsion in the deep region is relatively unimportant, as even physically changing d_d does not markedly change selectivity, Fig. 2B.

To approximate the decrease in d_s due to electrostatic repulsion, we examine the DNA effective diameter and the the distance from the wall at which the electric potential reaches thermal voltage, 26 mV. When we decrease the buffer ionic strength, two effects occur: the charge density on the DNA increases and the Debye length increases. Stigter *et al.* quantified these effects and derived a quantity known as the ''effective diameter''[10], which can be used to approximate the distance DNA can approach another negatively charged object. Based on X-ray crystallography, the physical diameter of DNA is around 2 nm [13]. Using Stigter's model, changing from TBE 5 × to TBE 0.25 × increases the DNA effective diameter from approximately 5.3 to 19 nm [10]. We do not take into account the differences in the persistence length of DNA in different ionic strengths, as it is shown not to change significantly under these conditions [14]. We ignore DNA length extension in nanochannels due to self-avoidance, as the DNA sizes explored here are rod-like unlike those examined by Reisner *et al.* [15].

Using wall ζ potentials measured by Pennathur and Santiago for the nanofilter oxide walls [16], the distance until 26 mV from the nanofilter wall is 0.5 nm for TBE 5 × and 5.0 nm for TBE 0.25 ×. When we model the DNA as a pill shape, the repulsion from the walls decreases d_s by $(19-5.3)+2*(5-0.5) \approx 20$ nm. Then, the effective shallow region depth of the $d_s = 85$ nm device is decreased to $d_{s,\text{effective}} \approx 85 - 20\,\text{nm} = 65$ nm. To summarize, decreasing the buffer ionic strength increased the extent of the electrostatic repulsion between the DNA molecules and the nanofilter walls. This repulsion effectively decreased the size of the nanofilter shallow region, resulting in increased selectivity.

As mentioned in Section 3.1, the relative mobility μ^* of DNA through the nanofilter array can be approximated to first order by the partition coefficient in the shallow region, K_s. Then selectivity is primarily determined by the shallow region depth. In our experiments the selectivity of the $d_s = 85$ nm nanofilter device run with TBE 0.25 × ($d_{s,\text{effective}} \approx 65$ nm) is comparable to that of a $d_s = 60$ nm nanofilter device run with TBE 5 ×: for each, the relative mobility μ^* reaches approximately 0.1 for 400 bp DNA.

The selectivity increase resulting from the decrease in buffer ionic strength caused the resolution to improve significantly. We define the separation resolution as the difference in elution time of two populations divided by half of the sum of the two peaks' widths. The separation resolutions for 400 and 500 bp DNA were 2.0 for TBE 5 ×, 3.4 for TBE 1 ×, and 4.2 for TBE 0.25 ×. For the TBE 5 × buffer, 100 and 200 bp DNA could not be resolved. Lowering the buffer ionic strength resulted in baseline resolution between these two peaks, Fig. 3A.

We note that decreasing the ionic strength to TBE 0.1 × and below resulted in difficulties getting the DNA to enter the nanofilter regions with depth d_s for the $d_s = 85$ nm device. This effect may be a result of charge-selectivity

effects exhibited by nanochannels at low ionic strengths [17]. Additionally, we note that electroosmotic flow was greater in magnitude than electrophoresis for ionic strengths less than TBE 1.7 ×; therefore, in these experiments DNA moved toward the cathode [18].

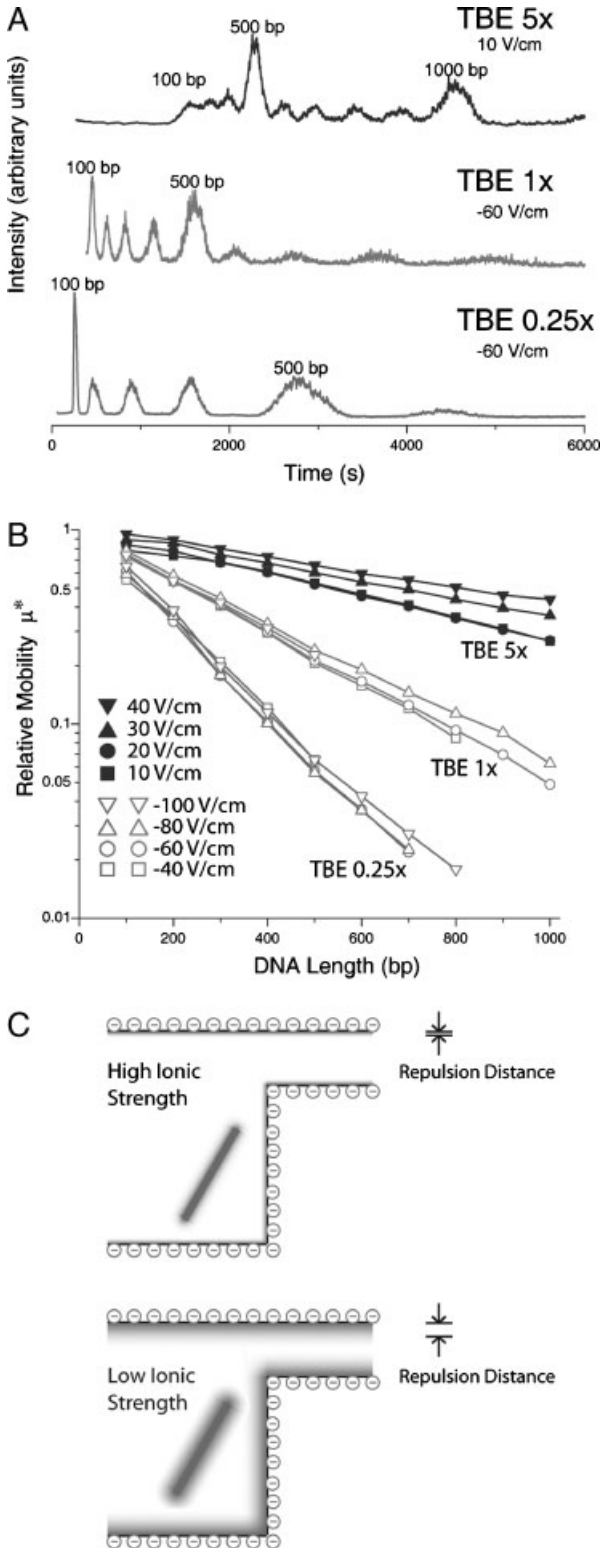

3.4 Selectivity in flat nanochannels

We performed control experiments in flat, filter-less nanofluidic devices to confirm that the selectivity increases in the nanofilter devices at lower buffer ionic strength are due to the presence of the nanofilters and not simply the presence of a nanochannel. These flat, filter-less devices have a constant channel depth of $d_s = d_d = 80$ nm. Our electrophoresis experiments showed no appreciable separation under similar buffer ionic strength conditions for DNA in a comparable size range, Fig. 4. Even when buffer ionic strength was decreased to TBE 1 ×, no baseline separation could be observed. An insufficient amount of DNA entered the separation channel at TBE 0.25 ×, resulting in fluorescence intensity too weak to detect at the observation point; therefore, results were not obtained. This effect may be similar to that experienced with a 40 nm shallow region nanofilter array, where the energy barrier to enter the shallow region was too high for a sufficient number of molecules to enter. These results confirm that the presence of alternating deep and shallow regions is necessary to achieve the enhanced selectivity obtained at lower buffer ionic strength.

Although other groups have demonstrated DNA separation in flat nanochannels, their DNA size ranges were different from ours. Pennathur *et al.* have demonstrated separation of DNA in the size range of 10–100 bp in flat nanochannels caused by inherent mobility differences and a process similar to hydrodynamic chromatography [19]. Specifically, smaller DNA in this size range exhibit somewhat smaller free-solution electrophoretic mobility than larger DNA in this size range, while this effect is much less apparent in the size range of 100–1000 bp DNA [9]. Also, 10–100 bp DNA have end-to-end lengths of 3–31 nm, while 100–1000 bp DNA have end-to-end lengths of 31–170 nm, using Eq. (1) and a rise/bp of 0.34 nm. With a nanochannel height of around 50 nm, the DNA of different sizes in the range 10–100 bp may indeed occupy different streamlines, resulting in separation. On the other hand, DNA of different sizes in the range 100–1000 bp are relatively larger and most likely occupy all streamlines equally.

Craighead and coworkers showed mobility differences during electrophoresis for 2–10 kbp DNA in a flat nanochannel purportedly caused by friction with the walls [20], which depends on the surface area of the molecules in contact with the walls. Configurations of 2–10 kbp DNA resemble a worm-like chain, as opposed to that of 100–1000 bp DNA, which

◀ **Figure 3.** Effect of buffer ionic strength on separation selectivity. The dimensions of the device were $d_s = 85$ nm, $d_d = 320$ nm, $p = 1$ μm. (A) Electropherograms measured at 1 cm. Different concentrations of TBE were created by diluting TBE 5 ×. (B) Relative mobility *versus* size for different buffer ionic strengths. The standard deviations of the mobility are all less than 9%, with most ranging from 5 to 7%, and are hence not included in the figure. (C) Decreasing the buffer ionic strength increases the distance over which electrostatic repulsion is felt between the negatively charged DNA and negatively charged walls.

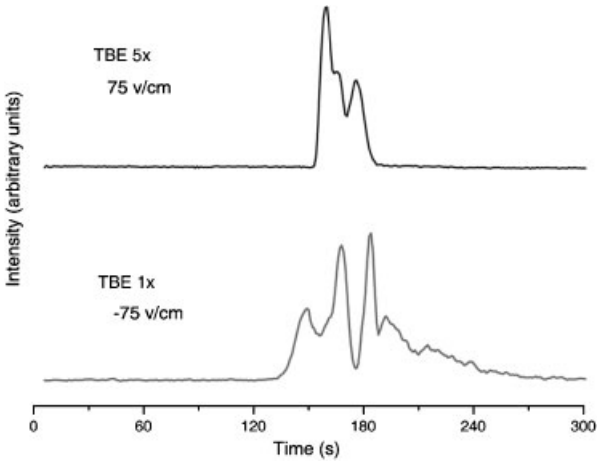

Figure 4. Electropherograms measured at 1 cm in a $d_s = d_d = 80$ nm device.

resemble rods. In Craighead's work, multiple segments of the DNA strand may touch the wall simultaneously, while in ours only the ends can touch the wall. Therefore, the friction effects are not as relevant to the size range of DNA we used, and our results show that baseline separation could not be achieved in a flat nanochannel.

4 Concluding remarks

In this work, we showed that decreasing buffer ionic strength in the nanofilter array led to higher selectivity and separation resolution for 100–1000 bp DNA. The cause of this increase in selectivity is consistent with the increased electrostatic repulsion between the negatively charged DNA and the negatively charged walls of the nanofilter device. The result is an effective decrease in the nanofilter constriction size caused by electrostatic repulsion. The conclusions of this work can be applied to extend the fabrication-related limits of the nanofilter arrays in separating even smaller molecules, such as peptides and carbohydrates. Since it is well established that one can reliably fabricate nanochannels with critical dimensions down to 20–40 nm, the result of this work would provide additional means to control the effective filter (pore) size down to a truly nanometer scale. While the ''repulsion distance'' was controlled by changing the ionic strength in this work, it would be also possible to achieve the same effect by changing the surface potential directly [21, 22]. This idea could be applied to nanofluidic systems and molecular nanofilters that require truly nanometer-scale sieving properties.

This work was supported by the Singapore–MIT Alliance and the DuPont–MIT Alliance. The authors thank Walter Resiner for helpful suggestions..

The authors have declared no conflict of interest.

5 References

[1] Fu, J., Mao, P., Han, J., *Appl. Phys. Lett.* 2005, *87*, 2939021–2939023.

[2] Fu, J., Yoo, J., Han, J., *Phys. Rev. Lett.* 2006, *97*, 0181031–0181034.

[3] Mao, P., Han, J., *Lab Chip* 2005, *5*, 837–844.

[4] Malone, D. M., Anderson, J. L., *Chem. Eng. Sci.* 1978, *33*, 1429–1440.

[5] Pujar, N. S., Zydney, A. L., *Ind. Eng. Chem. Res.* 1994, *33*, 2473–2482.

[6] Smith, F. G., Deen, W. M., *J. Colloid Interface Sci.* 1983, *91*, 571–590.

[7] Hooper, H. H., Baker, J. P., Blanch, H. W., Prausnitz, J. M., *Macromolecules* 1990, *23*, 1096–1104.

[8] Fu, J., Schoch, R. B., Stevens, A., Tannenbaum, S. R., Han, J., *Nat. Nanotechnol.* 2007, *2*, 121–128.

[9] Stellwagen, N. C., Gelfi, C., Righetti, P. G., *Biopolymers* 1998, *42*, 687–703.

[10] Stigter, D., *Biopolymers* 1977, *16*, 1435–1448.

[11] Han, J., Craighead, H. G., *J. Vac. Sci. Technol. A* 1999, *17*, 2142–2147.

[12] Giddings, J. C., Kucera, E., Russel, C. P., Myers, M. N., *J. Phys. Chem.* 1968, *72*, 4397–4408.

[13] Bates, A., Maxwell, A., *DNA Topology*, Oxford University Press, Oxford 2005.

[14] Hagerman, P. G., *Annu. Rev. Biophys. Biomol. Struct.* 1988, *17*, 265–286.

[15] Reisner, W., Beech, J., Larsen, N., Flyvbjerg, H. *et al.*, *Phys. Rev. Lett.* 2007, *99*, 0583021–0583024.

[16] Pennathur, S., Santiago, J. G., *Anal. Chem.* 2005, *77*, 6782–6789.

[17] Wang, Y.-C., Stevens, A., Han, J., *Anal. Chem.* 2005, *77*, 4293–4299.

[18] Han, J., Craighead, H. G., *Anal. Chem.* 2002, *74*, 394–401.

[19] Pennathur, S., Baldessari, F., Santiago, J. G., Kattah, M. *et al.*, *Anal. Chem.* 2007, *79*, 8316–8322.

[20] Cross, J. D., Strychalski, E. A., Craighead, H. G., *J. Appl. Phys.* 2007, *102*, 0247011–0247015.

[21] Schasfoort, R., Schlautmann, S., Hendrikse, J., van den Berg, A., *Science* 1999, *286*, 942–945.

[22] Karnik, R., Fan, R., Yue, M., Li, D. *et al.*, *Nano Lett.* 2005, *5*, 943–948.

